SATB2 Overexpression Promotes the Proliferation, Migration and Invasion of Oral Squamous Cell Carcinoma by Up-Regulating NOX4

Jie Gao
Affiliated Stomatological Hospital of Nanjing Medical University
Ying Meng
Affiliated Stomatological Hospital of Nanjing Medical University
Xin Ge
Affiliated Stomatological Hospital Of Nanjing Medical University
Chen-xing Hou
Affiliated Stomatological Hospital of Nanjing Medical University
Qing-hai Zhu
Affiliated Stomatological Hospital of Nanjing Medical University
Yi-zhou Wang
Affiliated Stomatological Hospital of Nanjing Medical University
Li-fan Sun
Affiliated Stomatological Hospital of Nanjing Medical University
Chen-xing Wang
Affiliated Stomatological Hospital Of Nanjing Medical University
Huai-qi Li
Affiliated Stomatological Hospital of Nanjing Medical University
Tianzhu Zhang
Southeast University
Jin-Hai Ye (yejinhai@njmu.edu.cn)
Affiliated Stomatological Hospital of Nanjing Medical University https://orcid.org/0000-0002-3789-551X

Primary research

Keywords: Oral squamous cell carcinoma, prognosis, SATB2, proliferation, NOX4

Posted Date: September 4th, 2020

DOI: https://doi.org/10.21203/rs.3.rs-70824/v1

Abstract

Background: While atypical expression of special AT-rich sequence-binding protein 2 (SATB2) has been approved associated with tumor progression, metastasis and unfavourable prognosis in various carcinomas. However, in oral squamous cell carcinoma (OSCC), both the expressive state and associated functions of SATB2's are still undefined.

Methods: Real-time PCR, western blotting, and immunohistochemistry were used to examine SATB2 expression. In vitro experiments including Flow Cytometry, CCK8 assay, migration assay, wound-healing assay were used to investigate the effects of SATB2 on HN4 cell proliferation, migration and invasion ability. Additionally, an orthotopic implantation assay was performed in nude mice to confirm the effects of SATB2 in vivo. Furthermore, a genome wide siRNA knockdown experiment was performed to explore the potential downstream regulatory mechanism of SATB2 in OSCC.

Results: We found that , in clinical samples from a retrospective cohort of 58 OSCC patients, high expression of SATB2 is associated with poor prognosis of OSCC patients. In this study, we investigated SATB2 is highly expressed in OSCC tissues and cell lines ,which can promotes OSCC cells' proliferation, migration, invasion and tumor growth. Following a genome wide siRNA knockdown experiment, we identified NOX4, a bona fide downstream target of SATB2, which can partially suppress OSCC proliferation. Furthermore, NOX4 knockdown inhibits tumorigenicity, which can be rescued partially by ectopic expression of SATB2.

Conclusion: Our findings not only indicate overexpression of SATB2 triggers the proliferative, migratory and invasive mechanisms which are important in the malignant phenotype of OSCC, but also identify NOX4 as the downstream gene for SATB2. These findings indicate that SATB2 may play a key role in OSCC tumorigenicity and may be a future target for the development of new therapeutic regimens.

1. Background

Oral squamous cell carcinoma (OSCC) is one of the most common solid malignancies worldwide, accounting for approximately 90% of all oral and maxillofacial malignancies in both sexes. The presence of regional lymph node metastasis has been considered as a reliable indicator of the prognosis in OSCC patients [1]. Surgery is currently the most effective treatment, especially for initial tumor likely to spread, Which in turn develops local invasiveness and lymph node metastasis. In recent years ,the multidisciplinary sequential therapy strategy (including surgery, radiotherapy, chemotherapy, and biotherapy) has been used to treat OSCC, however, there has been no significant improvement in the 5-year survival rate of patients, especially in those with neck metastasis or at an advanced pathological stage. [2–4]

STAB2 (Special AT-rich sequence-bind 2) is a nuclear transcription factor that play a vital role in various biological functions, such as osteoblast differentiation and bone matrix formation. [5–6]. After examining protein expression patterns in human normal and cancer tissues, STAB2 was considered to be a tissue-

type specific protein [7] and other studies on its tumorigenic roles have found that it may act as both a tumor suppressor and promoter. For example, SATB2 is often overexpressed in breast cancer [8], while only expressed at low levels in colorectal cancer [9]. Until now, there have been limited studies on SATB2's role in OSCC, although it has been shown to be highly expressed in advanced HNSCC (Head and Neck Squamous Cell Carcionma) where it can promotes HNSCC cells' chemoresistance and governs HNSCC cell survival [10].

The localization of NOX4 (encoded by a 265 kb gene located on chromosome 11q14.2-q21) is cell-type specific and can be found in mitochondria, endoplasmic reticulum, nucleus, and focal adhesions [11]. Initially considered to be a kidney-specific protein [12], NOX4 has been detected in numerous other tissues including blood vessels, heart, liver, and neurons [13]. NOX4 has a regulatory role in various cellular functions such as angiotensin II-induced vascularization [14] and insulin-triggered glucose uptake [15]. Abnormal NOX4 expression is associated with a wide range of cancer types including pancreatic and gastric cancer [16, 17], melanoma and von-Hippel-Lindau- deficient renal cell carcinoma [18]. NOX4 has been reported as being involved in almost every process of tumor development. NOX4 generate ROS may influence OSCC tumorigenicity and provide novel observations on metastasis, invasion, DNA damage, epithelial-to-mesenchymal transition (EMT) as well as helping cancer cells develop resistance to chemotherapeutic agents and radiation[11]. In osteosarcoma cell lines, SATB2 enhances migration and invasion by regulating genes involved in cytoskeletal organization. Microarray analysis identification of genes differentially regulated by SATB2 included NOX4, which is up-regulated in sh-SATB2 cells [19]. In this study, we tried to clarify the potential molecular mechanisms that SATB2 promotes the proliferation, migration, and invasion of OSCC by targeting NOX4.

In this, we examined STAB2 expression in OSCC samples and cell lines and its clinicopathological significance, its biological roles in OSCC cell lines, and the proliferative capacities of SATB2-modified OSCC cell lines.

2. Materials & Methods

2.1 Ethics Statement

The protocol for this study was approved by the Institutional Review Board of Nanjing Medical University and all experiments were performed after obtaining written informed consent for OSCC clinical specimens.

2.2 Patient and Tissue Samples

Specimens were obtained from a retrospective cohort of 58 primary human OSCC cases seen from Jan. 2011 to Dec. 2014. 11 samples of normal oral mucosa tissues from other non-cancer surgeries during the same period were collected from patients who underwent surgical resection at the department of oral and maxillofacial surgery, Nanjing Medical University (Nanjing, China). These OSCC patients did not receive any preoperative treatment before surgery. 6 pairs of fresh clinical specimens (for use in RT-PCR and

Western blot) were collected from OSCC patients at the same department. Histological examination was performed by senior oral pathologists (according to the diagnosis by Chief Dr Song XL, the senior pathologist at the Affiliated Stomatological Hospital of Nanjing Medical University), and diagnosis made based on carcinoma cell features as seen under a microscope. Tumors were classified according to the International Union Against Cancer (UICC) tumor staging system. All fresh tissue samples were collected and immediately stored at -80 °C until further use.

2.3 Mice

Animal studies were performed in an Association for Assessment and Accreditation of Laboratory Animal Care International accredited SPF animal facility and all protocols approved by the Animal Care and Use Committee of the Animal Research Center, Nanjing Medical University.

2.4 Cell lines and culture

Human oral keratin cells (OKC) and three human HNSCC cell lines: HN4, HN6, SCC25 were purchased from American Type Culture Collection (ATCC). Cancerous cell lines were cultured in DMEM media (Invitrogen) supplemented with 10% FBS (Hyclone) and 100 units/ml penicillin and streptomycin (Sigma) in 5% CO_2 at 37 °C.

2.5 Immunohistochemistry

IHC staining was performed using the standard streptavidin–biotin–peroxidase complex method according to the manufacturers' protocol (Abcam, USA). Briefly, 4 mm tissue sections from representative paraffin blocks were deparaffinized in xylene and rehydrated using an ethanol gradient. Endogenous peroxidases were blocked with 3% hydrogen peroxide. Slides were heated for antigen retrieval in 10 mM sodium citrate retrieval buffer (0.01 M sodium citrate and 0.01 M citric acid, pH 6.0), at 95℃ for 5 minutes. Sections were blocked in 10% normal swine serum for 20 minutes and incubated with monoclonal rabbit primary antibody (anti-SATB2, 1:200 dilution; Abcam, USA), monoclonal rabbit primary antibody (anti-NOX4, 1:400 dilution; Abcam, USA), at 4 ℃ overnight. Specimens incubated with PBS instead of primary antibodies were used as negative controls. Sections were then incubated with secondary antibodies for 45 minutes at room temperature. Reaction products were developed by 3, 3'-diaminobenzidine solution with hydrogen peroxide, followed by hematoxylin counterstaining. Immunoreactivity was semi-quantitatively evaluated according to staining intensity and distribution using the immunoreactive score calculated as: intensity score × proportion score. As previously reported, the intensity score was defined as; 0 (negative), 1 (weak), 2 (moderate), or 3 (strong), and the proportion score was defined as; 0 (negative) 1 (<10%) 2 (11–50%), 3 (51–80%), or 4 (>80%), of total positive cells. The total score ranged from 0 to 12 and the immunoreactivity of each slide was categorized into three subgroups based on the final score: 0 (negative), 1–4 (low expression), and 4–12 (high expression).

2.6 RNA extraction and quantitative real-time PCR

Total RNA was extracted using TRIZOL Reagent (Invitrogen) and cDNA synthesized using a reverse transcription Polymerase Chain Reaction (RT-PCR) Kit (TaKaRa) according to the manufacturer's instructions. Quantitative real-time Polymerase Chain Reaction (qRT-PCR) was performed using SYBR Premix Ex TaqTM II PCR Kit (TaKaRa) and an ABI 7500HT PCR sequencer (Applied Bio-systems). Primers specificity was verified by dissociation curve analysis. Data was analyzed using ABI SDS v2.4 software (Applied Biosystems). All qRT-PCR reactions were performed in triplicate. The housekeeping gene GAPDH was used as an internal control.

2.7 Western blot analysis

Protein samples were extracted by RIPA (Beyotime, Shanghai, China). Equal amounts of protein lysate were separated by SDS–PAGE, transferred to a polyvinylidenedifluoride (PVDF) membrane (Millipore), then blocked with 3% BSA in Tris-buffered saline with 0.1% Tween 20 (TBS-T) for 1 h at room temperature. The blocked membrane was then incubated with polyclonal primary antibody against (SATB2/MOX4) overnight at 4 ℃, washed three times in TBS-T, then incubated with horseradish peroxidase (HRP)-conjugated secondary antibody for 1 h at room temperature. Antibody-labelled proteins were detected using an ECL western blot detection kit (Bio-Rad Laboratories, Hercules, CA, USA) and X-ray film (Kodar). Tubulin or GAPDH were used as loading controls.

2.8 Immunofluorescence on HN4 cells

Cells were seeded onto 12-mm coverslips in 24 well plates. After 24 h incubation cells were washed in cold PBS, fixed with 4% paraformaldehyde for 30 minutes at room temperature, then washed three times with cold PBS. Cells were blocked with 3% BSA and 0.1% Triton-100 for 1 h at 37°C, incubated with a SATB2 primary antibody (Abcam,1:200) overnight at 4 ℃, washed three times with cold PBS, and incubated with FITC-conjugated secondary antibodies for 1 h. Cells were subsequently stained with DAPI for 10 min at room temperature (Roche Diagnostics), sealed with 70% glycerin, and examined using a Nikon fluorescence microscope.

2.9 Lentivirus generation and cell transfection

Lentivirus encoding full-length human SATB2 cDNA was purchased from Shanghai Cyagen biotechnology Co. Ltd. and used to transduct HN4 and HN6 cell lines which had reached 50% confluency. These cells were grown in DMEM medium (Invitrogen) with 10% FBS (Hyclone) for another 48h, after which stable SATB2 –expressing clones were screened by adding 10 μg/ml puromycin (Sigma) and growing for a further 24 hours. This was repeated twice to acquire Lv-SATB2-HN4 cells and N.C-transducted cells were used as controls.

2.10 siRNA Synthesis and Transfection

Specific small interfering RNAs (siRNA) against SATB2 and NOX4 were purchased from Shanghai Genepharma biotechnology Co. Ltd. One day before transfection, 2×10^5 HN4 cells (in 2ml antibiotic-free

growth medium) were seeded at per well in a 6-well plate (Costar) . The second day , each of 5μL siRNA vector (100ng/μL) or 3μL Lipofectamine ^{TM} 2000 (Invitrogen) were diluted in 50μL serum-free Opti-MEM medium (GIBCO,USA), mixed gently and incubated at room temperature for 5 min. Then, the diluted siRNA vector and Lipofectamine ^{TM} 2000 were combined, gently mixed, and incubated at room temperature for 20 minutes. During this incubation time, the seeded HN4 cells were washed twice with PBS and 1.9ml serum-free medium was added to each well. 100μL of the siRNA- Lipofectamine ^{TM} 2000 mixture was added to each well and gently mixed by rocking the plate. The cells were grown in 5% CO_2 and 95% air at 37℃ for 6 hours and the serum-free medium was exchanged for serum containing medium. Cells were grown for a further 72 h then collected for assays. The siRNA sequences are listed in Supplementary Table 4.

2.11 Flow Cytometry

HN4 and Lv-SATB2 –HN4 cells were trypsinized and resuspended in PBS. For cell cycle analysis, cells were washed in PBS for 3 times, fixed in 70% ethanol, and then stained with propidium iodide following RNase treatment. The DNA content and cell cycle distributions were analyzed using FACS flow cytometry (BD, USA) and Cell Quest software (BD Biosciences, USA).

2.12 CCK8 assay

Cell proliferation and viability were assessed using a CCK8 assay. $1x10^3$ cells were seeded in the wells of a 96-well plate and incubated overnight at 37°C. 10μl CCK8 was mixed with 90μl DMEM medium (Invitrogen) containing 10% FBS (Hyclone), and added to each well and plates were incubated for another 2-4 h. These steps were conducted in a dark environment. After 2-4 hours' incubation, we restarted time points (0, 24, 48 and 72 h), the absorbance was measured at 450 nm using an automatic enzyme-linked immune sorbent assay reader (Molecular Devices, San José, CA, USA).

2.13 Cell Migration and Invasion Assays

In wound healing experiments, cells were seeded at 70% confluency in 6-well plates (Costar) filled with DMEM/F -12 containing 10% FBS. 24 hours after seeding, scraped a wound line with a P1000 pipette tip among the confluent monolayers, washed to remove cell debris, and media was replaced. At specific time points, cells were fixed in 3.7% paraformaldehyde and photographed under a phase-contrast microscope. Migration assays were performed using a trans-well chamber (Corning, NY, USA). $1×10^4$ cells (in 200 μL DMEM/F-12) were placed on the upper layer of a cell-permeable membrane and 500 μL DMEM/F-12 containing 10% FBS was placed in the lower chamber. Following an incubation period, the cells that had migrated through the membrane were stained. Matrigel matrix (BD, Billerica, MAUSA) was used to simulate a human basement membrane for the invasion assay. DMEM and Matrigel matrix were mixed and the membrane was also coated with matrigel (1:9 dilution ratio) for testing invasion.

2.14 OSCC tumor xenograft formation in nude mice

All animal protocols used in this study were in accordance with the institutional animal welfare guidelines of Nanjing Medical University. Mice were randomly assigned into four groups, each containing six 4-to-6-week-old male nude mice. For HN4 cell line, each experimental group was subcutaneously injected with a total of 2×10^6 cells of either; HN4, Lv-SATB2-HN4, Lv-SATB2-HN4 with Negative Control, or Lv-SATB2-HN4 with NOX4 knockdown. As for HN6 cell line, each of 5×10^6 HN6 and Lv-SATB2-HN6 cells were subcutaneously injected into the left and right flanks respectively. Tumor sizes and weight were recorded every three days. All extant mice were euthanized at 4 or 8 weeks after injection then opened at injection sites to confirm tumor size and weight. Tumor volumes were measured by caliper and calculated as follows: Volume (mm^3) = $D \times d^2 \times 0.5$, where D is the longest, and d the shortest, diameter of the tumor.

2.14 Statistical analysis

All statistical analysis were performed using Graph Pad Prism 5.01 (La Jolla, CA, USA) or SPSS 18.0 (Armonk, NY, USA). Pearson χ^2 test was used to analyze the association between SATB2 expression and clinical pathology parameters. Survival rate analysis was analyzed by Kaplan–Meier plot and log-rank test. Independent Student t-test and ANOVA with post hoc test were used for most other analyses as indicated in figure legends. The data are presented as the mean ±S.D. of at least three independent experiments. The P-values were defined as *P□0.05, **P□0.001 and ***P□0.0001.

3. Results

3.1 SATB2 is overexpressed in OSCC samples and cell lines

Previous studies indicated that SATB2 could be a crucial oncogenic gene during cancer development and progression [7, 9]. To examine SATB2 expression in primary OSCC, we first assessed the expression of SATB2 protein in the clinical specimens retrieved from 58 primary OSCC patients by immunohistochemical staining. Representative immunohistochemical staining of primary OSCC and normal oral mucosa is shown in Fig. 1A. SATB2 protein abundance in these primary OSCC (n = 58) and normal oral mucosa specimens (n = 11) was categorized according to our immunohistochemistry scoring regime. SATB2 levels in the OSCC specimens were graded as negative (0), low (18) and high (40) expression and in the normal samples were graded as negative (9), low (2) and high (0) (Table 1), indicating that it was overexpressed in the majority of clinical samples. SATB2 was highly expressed in the majority of OSCC specimens (31 of 42) with advanced pathological staging (□-□), whereas only a minority (7 of 16) of lower-stage (□-□) tumors showed elevated expression. (Fig. 1B, P/0.05).

To support these observations, mRNA from six pairs of fresh oral carcinoma tissues including tongue, gingiva, palate, and the para-carcinoma tissues of the corresponding sites were analyzed by RT-PCR. The mRNA levels of SATB2 were significantly increased in tumor group compared to the control (Fig. 1C). Western blots for SATB2 in the parallel samples also showed the increased expression in the tumor group compared to the control (Fig. 1D). We then assessed the expression profile of SATB2 in the human tongue (SCC25) and head and neck squamous cell lines (HN4 and HN6), with human oral keratin cells

(OKC) as the control and showed that SATB2 mRNA levels were higher in HN4, HN6, SCC25 compared to the OKC control (Fig. 1E). This result was further supported by western blotting using the HN4 cell line (Fig. 1F).

3.2 SATB2 overexpression is associated with tumor size, cervical node metastasis, clinical stage, and poor prognosis of OSCC

The epidemiologic information and relevant clinicopathological features of patients are summarized in Table 2. In brief, 37 male and 21 female patients were enrolled with mean age 56.5 years with a range of 39–79 years. The average follow-up period was 54.7 months. There were no significant correlations between SATB2 expression with patients' gender, age, and pathological grade, however, a Pearson χ^2 test revealed significant associations between SATB2 abundance and tumor size (P = 0.007), cervical nodes metastasis (P = 0.043) and clinical stage (P = 0.031). To examine any potential prognostic value in OSCC, we examined SATB2 expression and patient survival. At last follow-up with the 58 patient cohort, 35 (60.3%) were alive and disease-free, 6 (10.3%) were alive but had recurrence and/or cervical nodal metastasis, and 17 (29.4%) had died due to either a local recurrence, metastasis, or other unrelated reasons. The results from the Kaplan–Meier survival analyses indicated that high SATB2 expression had an adverse prognostic impact on patients' outcomes and was negatively related to overall survival (Fig. 1G, Log-rank, P = 0.0179).

3.3 Establishment of Lv-SATB2-HN4 and Lv-SATB2-HN6 cell lines

HN4 cells were transducted with the full-length human SATB2 cDNA to evaluate its function. Cells were screened twice with puromycin for 72 h post-transduction to ensure stable transduction had occurred. Green fluorescent protein was observed by fluorescence microscopy 48 h post-transduction (Fig 2A). Both SATB2 mRNA and protein levels were significantly increased in Lv-SATB2-HN4 and Lv-SATB2-HN6 cells compared to HN4 and HN6 cells. (Fig 2B). Immunofluorescence indicated that there was stronger immunocytochemical staining in Lv-SATB2-HN4 cells (Fig 2C). These results confirmed that a SATB2 modified-HN4 cell line was successfully established and ready for use in subsequent experiments.

3.4 SATB2 overexpression promotes HN4 and HN6 proliferation

To further investigate the biological role of SATB2 we used flow cytometry to examine the cell cycle profile of HN4 before and after SATB2 overexpression. The results showed that compared to HN4 cells, Lv-SATB2 cells had a significant decrease in the percentage of cells in G1 phase (HN4:63.33% ±2.44; Lv-SATB2: 51.37 % ±2.96), and an increase in the percentage of cells in S phase (HN4: 23.51% ±8.84; Lv-SATB2: 38.26 %±8.49) (Fig 3A). Cell proliferation was examined using a CCK-8 assay at 3 time points (24, 48, and 72 h) and was consistent with the cell cycle analysis, in that from 24 h, the number of viable cells was significantly higher in Lv-SATB2 than either HN4 and HN6 (Fig 3B). To further clarify SATB2's tumorigenic potential *in vivo*, HN4, Lv-SATB2-HN4, HN6, and Lv-SATB2-HN6 cells, were subcutaneously injected into the left armpit of the mice. Eight weeks after injection tumors were resected and collected. Tumor volumes and weights were markedly increased in the Lv-SATB2 groups compared to the control

groups (Fig 3C, D). The expression of key molecules that regulate the G1/S phase transition in HN4 and Lv-SATB2-HN4 cells was examined. Persistent SATB2 activation has been associated with the promotion of proliferation, anti-apoptosis, invasion, metastasis, angiogenesis, and immune escaping behaviors, and with genes encoding key cancer-promoting inflammatory mediators in most malignant tumor cells [20]. Interleukin-6 (IL-6), signal transducers and activators of transcription 3 (STAT3), and p-STAT3 levels in the cytoplasm of HN4 and Lv-SATB2 cells were determined by western blot (Fig 3E). The expression of IL-6 (the most important of STAT3 activators) was significantly increased after SATB2 overexpression. SATB2 overexpression in HN4 cells results in phosphorylation of Tyr705 in STAT3, leading to its nuclear translocation. STAT3-regulated genes encode cytokines, such as IL-6, which in turn activate the STAT3 signaling pathway and consequently propagate a feed-forward loop between tumor and immune cells in the tumor microenvironment [20].

3.5 SATB2 overexpression promotes HNSCC migration and invasion

Metastasis is a feature of most malignant tumors and the culprit of many cancer-related deaths. Previous reports demonstrated that SATB2 promoted head and neck squamous cells proliferation and their survival in the presence of radiation [10]. To explore the specific roles of SATB2 in OSCC metastasis, we examined their migration and invasion. SATB2 overexpression significantly enhance both cell migration, as evidenced by wound-healing and transwell assays, compared to the control cells (Fig. 4A-C) and invasion in the transwell matrigel invasion assays (Fig. 4D). SATB2 overexpression in HN4 cells promoted tumor lung metastasis in one mouse (Fig. 4E), which provided direct evidence to support the hypothesis that SATB2 contributed to cell invasion.

The epithelial-mesenchymal transition (EMT) has been reported as an important biological process in embryonic development and tumorigenesis [21]. During this process, epithelial tumor cells can obtain mesenchymal phenotypes and promote tumor invasion and metastasis. We detected E-cadherin (epithelial marker) and vimentin (mesenchymal marker) protein levels by western blotting in HN4 and Lv-SATB2-HN4 cells. Our data showed decreased expression of E-cadherin and increased expression of Vimentin in Lv-SATB2-HN4 cells compared to their counterparts (Fig 4. F). Collectively, these results indicate that SATB2 overexpression promotes HNSCC migration and invasion both *in vitro* and *in vivo*, as well as facilitates the epithelial-mesenchymal transition of OSCC cells.

3.6 NOX4 is up-regulated after SATB2 overexpression in HN4 cells

NOX4 knockdown by siRNAs reduces cell proliferation and inhibits OSCC tumor growth.

We analyzed NOX4 expression levels in HN4 and Lv-SATB2-HN4 cells (n=3). The results showed that NOX4 was significantly up-regulated in Lv-SATB2-HN4 compared to HN4 cells by RT-PCR (Fig 5A), western blot (Fig 5B) and immunofluorescence (Fig 5C).

To better understand the function of NOX4, three NOX4-specific siRNAs (si-NOX4) were designed to selectively deplete NOX4. Cells treated with scrambled si-RNA were used as small interfering-non-target

controls (si-NC). The results from RT- PCR, western blot, and immunofluorescence assays demonstrated successful inhibition in the si-NOX4 group compared to the si-NC group (Fig. 5D-F). Cell proliferation was detected by a CCK-8 assay after 24h, 48h and 72h. The number of viable cells markedly decreased in the siNOX4-treated cells compared to the control and the differences were statistically significant at 72 h (Fig 5G). Cell cycle distribution among cells was determined by flow cytometry to further investigate NOX4's effect on cell growth. We found that NOX4 down-regulation induced cell cycle arrest at the G1/S checkpoint (Fig 5H, Table 3). These results indicate that NOX4 plays an important role in tumor formation in Lv-SATB2-HN4 cells and can be a positive regulator of tumor growth. To investigate NOX4's *in vivo* tumorigenic potential , scrambled siRNA and siNOX4-treated cells were subcutaneously engrafted in the left armpit of mice, respectively. To minimize the number of mice used, three NOX4-specific siRNAs-treated cells were equally mixed together as the siNOX4 group. NOX4 knockdown could effectively suppress tumor initiation when compared to the control group (Fig 5I).

4. Discussion

In our previous study, our study confirmed the inhibition of miR-34a in the invasion, proliferation, and migration of the OSCCs, playing a potential tumor suppressor role with SATB2 as its downstream target [22]. In this study, we further investigated the expression pattern of SATB2 in OSCC. SATB2 overexpression was significantly associated with tumor size, cervical node metastasis, and clinical stage, all of which have critical clinicopathological relevance and prognostic significance for OSCC patients. We also observed prominent expression of SATB2 in OSCC tissues compared with para-carcinoma oral tissues. SATB2 overexpression in HN4 cells promoted proliferation, migration, and invasion, as well as facilitating EMT and activating the Janus kinase (JAK)/STAT3 signaling pathway. These findings suggest that SATB2 overexpression in important for progression in oncogenesis, like the role of SATB1 in breast cancer [23]. Because of the limited number of patients enrolled in this study, more patients from multiple institutions are needed to definitively establish SATB2's overexpression pattern as well as its diagnostic utility in OSCC.

In this study, our findings support that hypothesis that SATB2 has influence on the determination of OSCC proliferation, migration, invasion, and tumor growth *in vitro* and *in vivo*. In future experiments, we aim to examine the expression of key molecules that regulate the G1/S phase transition in HN4 cells and Lv-SATB2-HN4 cells.

In Lv-SATB2-HN4 cells, high levels of IL-6 and p-STAT3 have been discovered, but total STAT3 expression is stable. Phosphorylated STAT3 is a nuclear transcription factor involved in tumor proliferation, survival, angiogenesis, and invasion, in addition to influencing genes encoding key cancer-promoting inflammatory mediators [20, 24]. IL-6 has been described as acting like a cytokine and activates STAT3 phosphorylation signaling. Obviously, STAT3 activation can be achieved via other signaling pathways, such as receptor-tyrosine kinases, which are dysregulated in cancer. It has been reported that IL-6 promotes head and neck tumor metastasis and EMT via the STAT3/SNAIL signaling pathway [24]. Like

SATB1 in breast cancer [23], IL-6 promotes growth and invasion of breast cancer cells through STAT3-dependent up-regulation of the NOTCH signaling pathway [20, 24, 25].

Previous studies have suggested that knocking down, or silencing, NOX4 caused increased cell proliferation in hepatocytes and hepatocarcinoma cells and *in vivo*, suggesting that it suppresses liver cell proliferation [26]. Our findings show that NOX4 was prominently expressed in lentiviral transducted SATB2-specific HN4 cells, and that silencing expression using NOX4-targeted siRNA decreased viability of HN4 cells. In this study, the involvement of NOX4 in proliferation had been confirmed by CCK-8 assay and Flow Cytometry. NOX4 appears to be a constitutively active enzyme that is transcriptionally regulated [11]. As a key oxygen sensor, NOX4-derived H_2O_2 plays diverse roles in cell proliferation, migration, and death. Increased NOX4 expression has been observed in cancer, which ptomotes in metastasis, angiogenesis, DNA damage, anti-apoptosis and EMT [27].

In future experiments, we will investigate these areas and examine whether there is a direct association between SATB2 and the NOX4 promoter.

5. Conclusion

Our study shows that OSCC patients with high SATB2 levels usually have poorer prognosis. In both *in vitro* and *in vivo*, SATB2 overexpression promotes proliferation, partially via up-regulating NOX4, and enhanced migration and invasion of OSCC cells. Our findings suggest that SATB2 could not only serve as a novel and viable biomedical diagnostic and prognostic biomarker, but also may be a potential therapeutic target in OSCC.

Abbreviations

SATB2: AT-rich sequence-binding protein 2; OSCC: oral squamous cell carcinoma; HNSCC: Head and Neck Squamous Cell Carcionma; UICC: International Union Against Cancer; EMT: epithelial-to-mesenchymal transition; OKC: oral keratin cells; ATCC: American Type Culture Collection;RT-PCR: Reverse Transcription-Polymerase Chain Reaction; TBS-T: Tris-buffered saline with 0.1% Tween 20 ; PVDF: polyvinylidenedifluoride ; qRT-PCR: Quantitative real-time Polymerase Chain Reaction ; HRP: horseradish peroxidase; siRNA: small interfering RNAs; IL-6: Interleukin-6; STAT3: signal transducers and activators of transcription 3;si-NOX4: NOX4- specific siRNAs; si-NC: Small interfering-non-target controls; JAK: Janus kinase;

Declarations

Ethics approval and consent to participate

The study which including human and animal approval were acquired from the Ethics Committee of The Affiliated Stomatology Hospital of Nanjing Medical University .All experiments were performed after obtaining written informed consent for OSCC clinical specimens.

Consent for publication

We assure that the material is original and it has not been published elsewhere yet.

Data availability statement

All datasets presented in this study are included in the article/additional files.

Acknowledgements

We acknowledged and appreciated the colleagues for their valuable comments on this paper.

Authors' contributions

J. G and J.-h. Y.conceived and designed the experiments. J. G. , Y. M. , and G. X. performed the experiments. Q.-H. Z. , C.-X. H., Y.-Z. W. , L.-F. S. , C. -X. W. and H.-Q. L. analyzed the data. J. G. , X. G. , Y. M. and J.-h. Y. contributed to the writing and critical reading of the paper. All authors read and gave their approval for the final version of the manuscript.

Funding

This research was funded by the National Natural Science Foundation of China: 81371123, Priority Academic Program Development of Jiangsu Higher Education Institutions: PAPD, 2018- 87, Qing-Lan Project: JX2161015067, Jiangsu Provincial Medical Key Talent Project: ZDRCA2016087, the Southeast University-Nanjing Medical University Cooperative Research Project: JX105GSP2017DN03, Jiangsu Provincial Medical Innovation Team: CXTDA2017036.

Competing interests

The authors declare that the research was conducted in the absence of any commercial or financial relationships that could be construed as a potential conflict of interest.

References

1. Scully C,Bagan J. Oral squamous cell carcinoma overview. Oral Oncol,2009;45(4-5): 301-308.
2. Monteiro LS, Amaral JB, Vizcaino JR, Lopes CA, Torres FO. A clinical-pathological and survival study of oral squamous cell carcinomas from a population of the North of Portugal. Med. Oral Patol. Oral Cir. Bucal 2014;19(2):e120–e126.
3. Brands MT, Brennan PA, Verbeek ALM, Merkx MAW, Geurts SME. Follow-up after curative treatment for oral squamous cell carcinoma. A critical appraisal of the guidelines and a review of the literature. Eur J Surg Oncol; 2018;44(5):559-565.
4. Rodrigo JP, Grilli G, Shah JP, Medina JE, Robbins KT, Takes RP, et al. Selective neck dissection in surgically treated head and neck squamous cell carcinoma patients with a clinically positive neck

Systematic review. Eur J Surg Oncol; 2018;44(4):395-403.

5. Hassan MQ, Gordon JAR, Beloti MM, Croce CM, van Wijnen AJ, Stein JL, et al. A network connecting Runx2,SATB2, and the miR-23a~27a~24-2 cluster regulates the osteoblast differentiation program. Proc Natl Acad Sci USA, 2010, 107(46): 19879–19884.
6. Dobreva G, Chahrour M, Dautzenberg M, Chirivella L, Kanzler B, Fariñas I, et al. SATB2 is a multifunctional determinant of craniofacial patterning and osteoblast differentiation. Cell, 2006, 125(5): 971–986
7. Perez Montiel D, Arispe Angulo K, Cantú-de León D, Bornstein Quevedo L, Chanona Vilchis J, Herrera Montalvo L. The value of SATB2 in the differential diagnosis of intestinal-type mucinous tumors of the ovary: primary vs metastatic. Ann Diagn Pathol. 2015;19(4):249-52.
8. Patani N, Jiang W, Mansel R, Newbold R, Mokbel K. The mRNA expression of SATB1 and SATB2 in human breast cancer. Cancer Cell Int. 2009; 9:18.
9. Wang S, Zhou J, Wang XY, Hao JM, Chen JZ, Zhang XM, et al. Down-regulated expression of SATB2 is associated with metastasis and poor prognosis in colorectal cancer. J Pathol, 2009, 219(1): 114–122.
10. Chung J, Lau J, Cheng LS, Grant RI, Robinson F, Ketela T, et al. SATB2 augments ΔNp63α in head and neck squamous cell carcinoma. EMBO Rep, 2010, 11(10): 777–783
11. Guo S, Chen X. The human Nox4: gene, structure, physiological function and pathological significance. J Drug Target, 2015; 23(10): 888–896
12. Geiszt M, Kopp JB, Várnai P, Leto TL. Identification of renox, an NAD(P)H oxidase in kidney. Proc Natl Acad Sci U S A; 2000;97(14):8010-8014.
13. Mochizuki T, Furuta S, Mitsushita J, Shang WH, Ito M, Yokoo Y, et al. Inhibition of NADPH oxidase 4 activates apoptosis via the AKT/ apoptosis signal-regulating kinase 1 pathway in pancreatic cancer PANC-1 cells. Oncogene. 2006;25(26):3699-3707.
14. Yamaura M, Mitsushita J, Furuta S, Kiniwa Y, Ashida A, Goto Y, et al. NADPH oxidase 4 contributes to transformation phenotype of melanoma cells by regulating G2-M cell cycle progression. Cancer Res. 2009; 69(6):2647–54
15. B Lassègue, D Sorescu, K Szöcs, Q Yin, M Akers, Y Zhang, S L Grant, et al. Novel gp91(phox) homologues in vascular smooth muscle cells: nox1 mediates angiotensin II-induced superoxide formation and redox-sensitive signaling pathways. Circ Res. 2001; 88(9):888-894.
16. Mahadev K, Motoshima H, Wu X, Ruddy JM, Arnold RS, Cheng G, et al. The NAD(P)H oxidase homolog Nox4 modulates insulin-stimulated generation of H_2O_2 and plays an integral role in insulin signal transduction. Mol Cell Biol. 2004; 24(5):1844-1854.
17. Vaquero EC, Edderkaoui M, Pandol SJ, Gukovsky I, Gukovskaya AS. Reactive oxygen species produced by NAD(P)H oxidase inhibit apoptosis in pancreatic cancer cells. J Biol Chem. 2004; 279(33):34643-54.

18. Tang CT, Lin XL, Wu S, Liang Q, Yang L, Gao YJ, et al. NOX4-driven ROS formation regulates proliferation and apoptosis of gastric cancer cells through the GLI1 pathway. Cell Signal. 2018; 46:52-63.
19. Maranchie J K, Zhan Y. Nox4 is critical for hypoxia-inducible factor 2-alpha transcriptional activity in von Hippel-Lindau-deficient renal cell carcinoma. Cancer Res. 2005; 65(20): 9190- 9193.
20. BKA Seong, J Lau, T Adderley, L Kee, D Chaukos, M Pienkowska, et al. SATB2 enhances migration and invasion in osteosarcoma by regulating genes involved in cytoskeletal organization. Oncogene. 2015;34(27):3582-3592.
21. Yu H, Kortylewski M, Pardoll D. Crosstalk between cancer and immune cells: role of STAT3 in the tumour microenvironment. Nat Rev Immunol. 2007; 7(1):41-51.
22. Lamouille S, Xu J, Derynck R. Molecular mechanisms of epithelial-mesenchymal transition. Nat Rev Mol Cell Biol. 2014; 15(3):178-96.
23. Ge X, Gao J, Sun QW, Wang CX, Deng W, Mao GY, et al. MiR-34a inhibits the proliferation, migration, and invasion of oral squamous cell carcinoma by directly targeting SATB2. J Cell Physiol. 235(5):4856-4864..
24. Han HJ, Russo J, Kohwi Y, Kohwi-Shigematsu T. SATB1reprogrammes gene expression to promote breast tumour growth and metastasis. Nature. 2008; 452(7184): 187–193.
25. Yu H, Pardoll D, Jove R. STATs in cancer inflammation and immunity: a leading role for STAT3. Nat Rev Cancer. 2009; 9(11):798–809
26. Yadav A, Kumar B, Datta J, Teknos TN, Kumar P. IL-6 promotes head and neck tumor metastasis by inducing epithelial-mesenchymal transition via the JAK-STAT3-SNAIL signaling pathway. Mol Cancer Res. 2011; 9(12):1658–1667.
27. Crosas-Molist E, Bertran E, Sancho P, López-Luque J, Fernando J, Sánchez A, et al. The NADPH oxidase NOX4 inhibits hepatocyte proliferation and liver cancer progression. Free Radic Biol Med. 2014; 69:338–347.
28. Przybylska D, Mosieniak G. The role of NADPH oxidase NOX4 in regulation of proliferation, senescence and differentiation of the cells. Postepy Biochem. 2014; 60(1): 69-76.

Tables

Table 1 The expression of SATB2 in human OSCC specimens and normal oral mucosa

	SATB2 expression			positive rate	χ^2	*P* values
	high	low	Negative			
OSCC （58）	39	19	0	100%	55.568	*<0.01*
normal oral mucosa(11)	0	2	9	18.1%		

The number in italic indicate statistical significance with *p* values <0.01

Table 2 Association between SATB2 expressions with key clinicopathological parameters in 58 OSCC specimens

Clinicopathological parameters	Cases	SATB2		$\chi 2$	*P-Values*
		Low	High		
Gender	58	19	39		
Male	37	13	24	0.262	>0.05
Female	21	6	15		
Age					
≤60	30	12	18	1.479	>0.05
>60	28	7	21		
Tumor size					
T1-T2	31	15	16	7.384	<0.05
T3-T4	27	4	23		
Pathological grade					
Ⅰ	33	14	19	3.247	>0.05
Ⅱ-Ⅲ	25	5	20		
Cervical node metastasis					
N(0)	30	14	16	5.457	<0.05
N(+)	28	5	23		
Clinical stage					
Ⅰ-Ⅱ	16	9	7	5.535	<0.05
Ⅲ-Ⅳ	42	10	32		

Table 3 Cell cycle distribution of SATB2 modified-HN4 cells (Lv-SATB2) after transfecting si-N.C and si-NOX4

	Lv-SATB2	si-N.C	si-NOX4-1	si-NOX4-2	si-NOX4-3
G1 (%)	56.7	53.46	89.04	93.58	96.11
S (%)	40.12	38.86	8.36	4.89	2.33
G2 (%)	3.18	7.68	2.60	1.53	1.57

Table 4 siRNA sequences of NOX4

human	sense (5'- 3')	antisense (5'-3')
NOX4-Homo-1	CCUCAGCAUCUGUUCUUAATT	UUAAGAACAGAUGCUGAGGTT
NOX4-Homo-2	GCAGGAGAACCAGGAGAUUTT	AAUCUCCUGGUUCUCCUGCTT
NOX4-Homo-3	CCCUCAACUUCUCAGUGAATT	UUCACUGAGAAGUUGAGGGTT

Figures

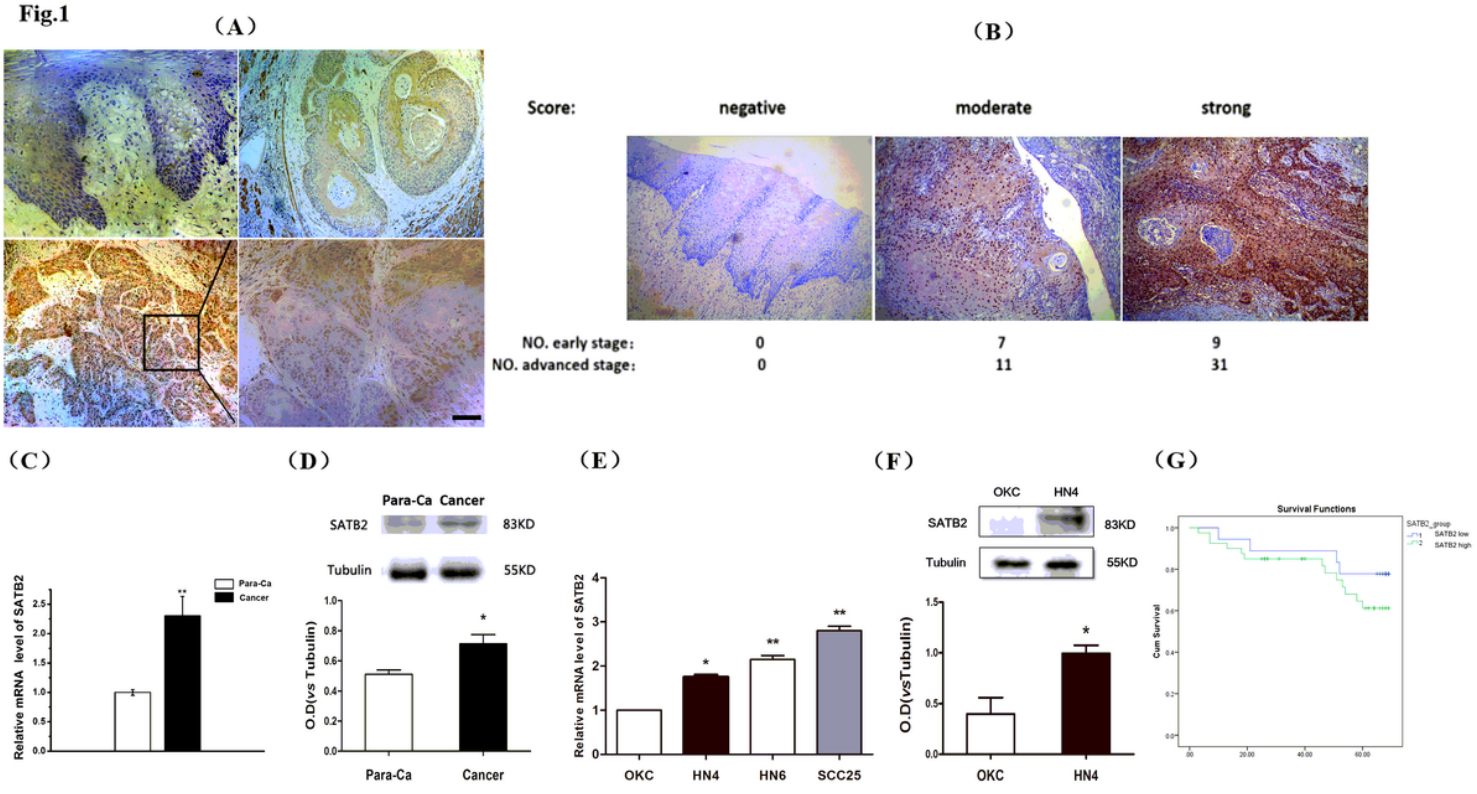

Figure 1

SATB2 is highly-regulated in OSCC tissues and is associated with patient prognosis. Fig1a. Representative weak staining of SATB2 (low expression) in normal human oral mucosa (×200). Nuclei are counterstained with haematoxylin. b Representative weak staining of SATB2 (low expression) in primary OSCC specimens (×200). c Representative strong staining of SATB2 (high expression) in primary OSCC specimens (×200). d This image is enlarged (x200) from the black box area in c. SATB2 expression is ascertained primarily in the nuclei of cancer cells. Scale bar 100 μm. Fig1B. 58 primary OSCC specimens immunostained with SATB2 antibody, scored as negative, moderate or strong. The numbers of early- and advanced-stage specimens (×100) are indicated under the representative images of each scoring category. Fig1C-D. SATB2 mRNA and protein levels measured by RT-qPCR in 6 pairs of OSCC tissue specimens compared to para-carcinoma tissue specimens. Fig1E. SATB2 mRNA levels measured by RT-qPCR in 3 OSCC cells compared to OKC cells Fig1F. SATB2 protein levels determined by WB in HN4 cells compared to OKC cells. Fig1G. High SATB2 expression is significantly associated with poor overall survival in primary OSCC patients. * $p < 0.05$, ** $p < 0.01$

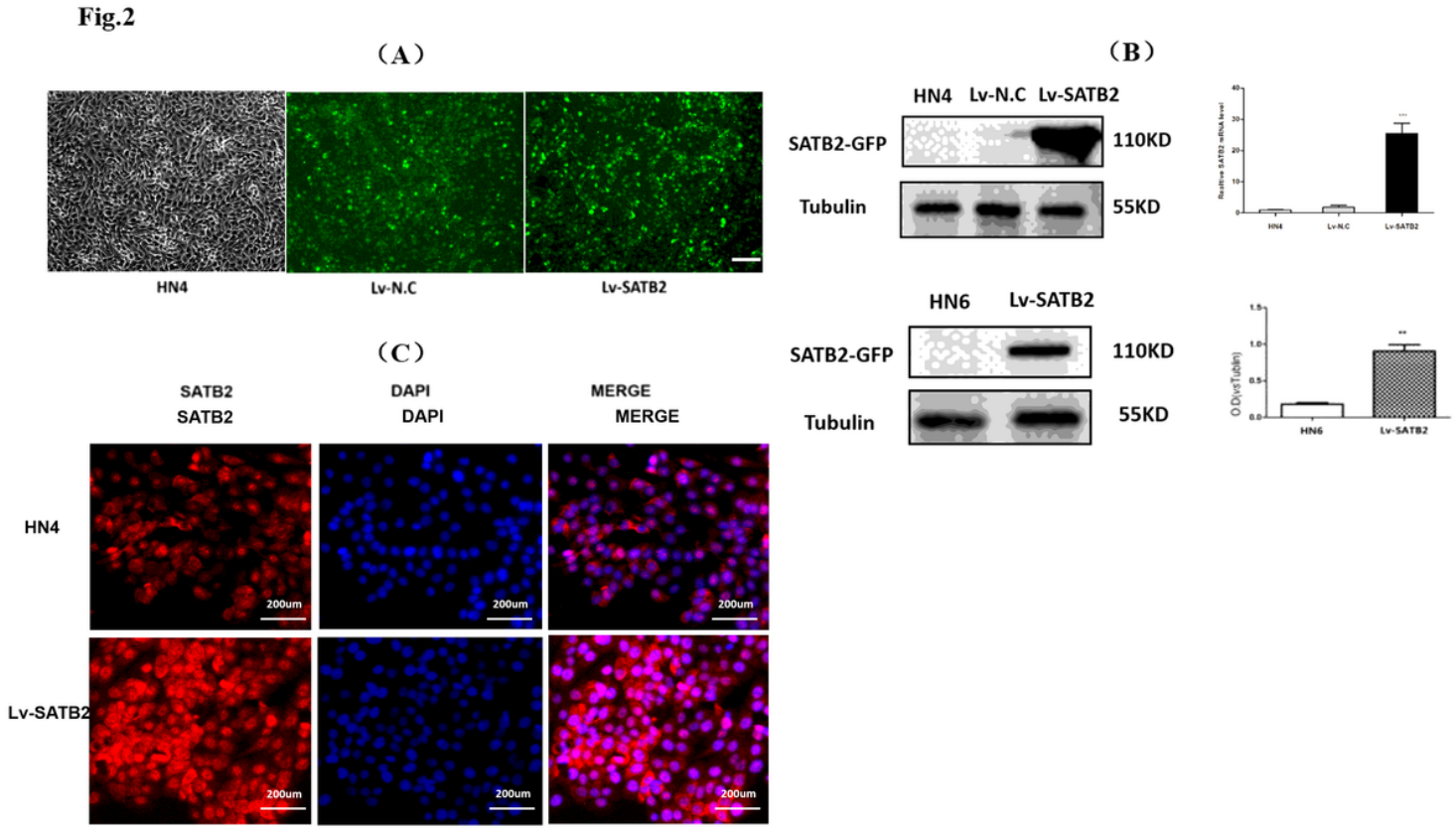

Figure 2

SATB2 mRNA and protein expression levels in HNSCC lentiviral transduction. Fig2A. Fluorescence images of HN4 cells transducted by lentivirus with SATB2. Fig2B. Relative SATB2 mRNA and protein levels in each group after transduction. Fig2C. Localization of SATB2 identified by immunofluorescence staining in HN4 and Lv-SATB2 cells ** p < 0.01,***p < 0.001

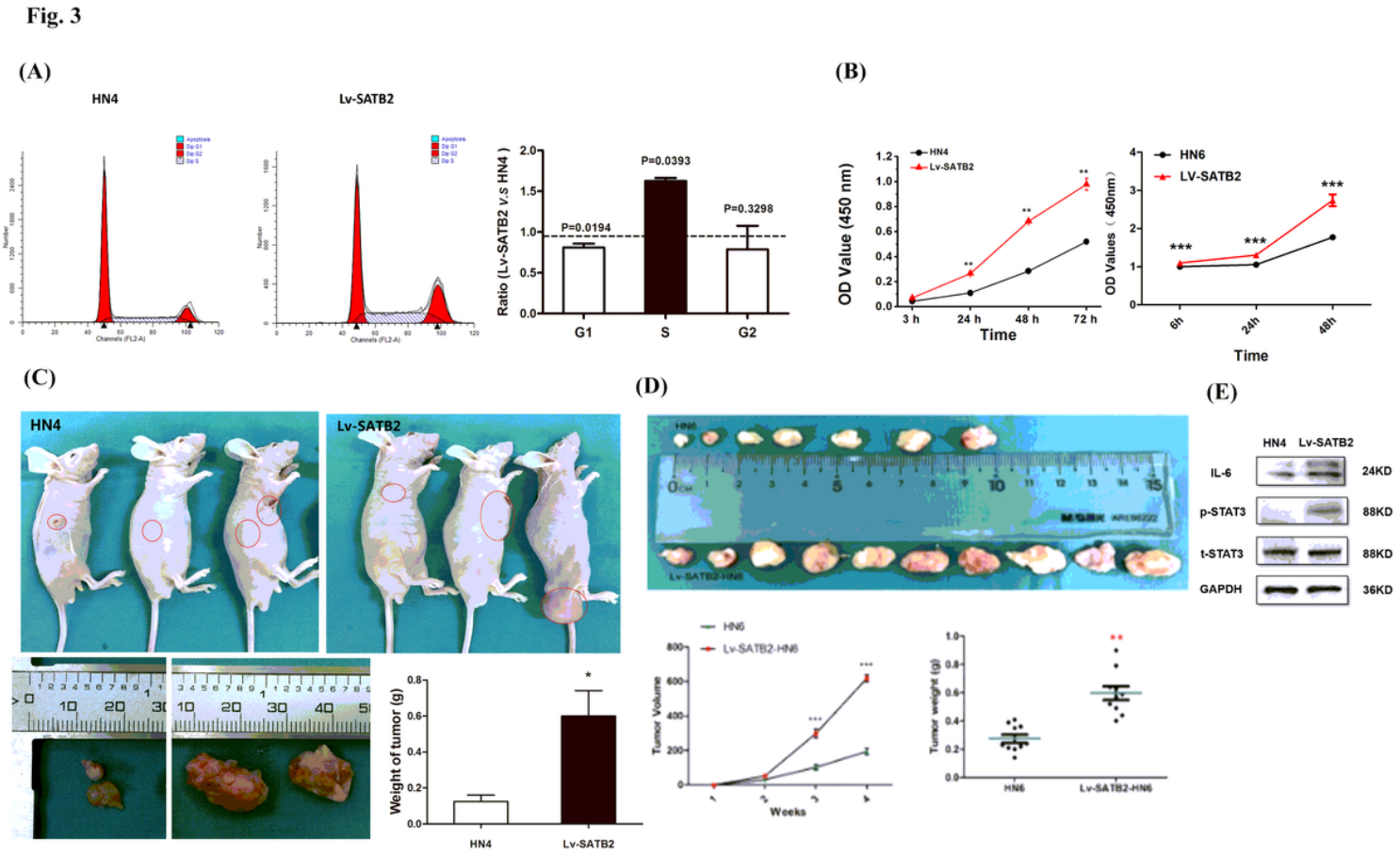

Figure 3

SATB2 promotes cell growth in HNSCC and initiates STAT3 signaling pathway phosphorylation. Fig3A. Cell cycle profile of HN4 and Lv-SATB2 cells determined by flow cytometry. Fig3B. The CCK8 assay shows that SATB2 promotes proliferation of both HN4 and HN6 cells. Fig3C. Tumor weight in samples harvested from mice bearing HN4 and Lv-SATB2 cells after 8 weeks' growth. Fig3D. Tumor weight in samples harvested from mice bearing HN6 and Lv-SATB2 cells after 8 weeks' growth. Fig3E.IL-6, STAT3, p-STAT3 levels in HN4 and Lv-SATB2 cells determined by WB. * p < 0.05, ** p < 0.01

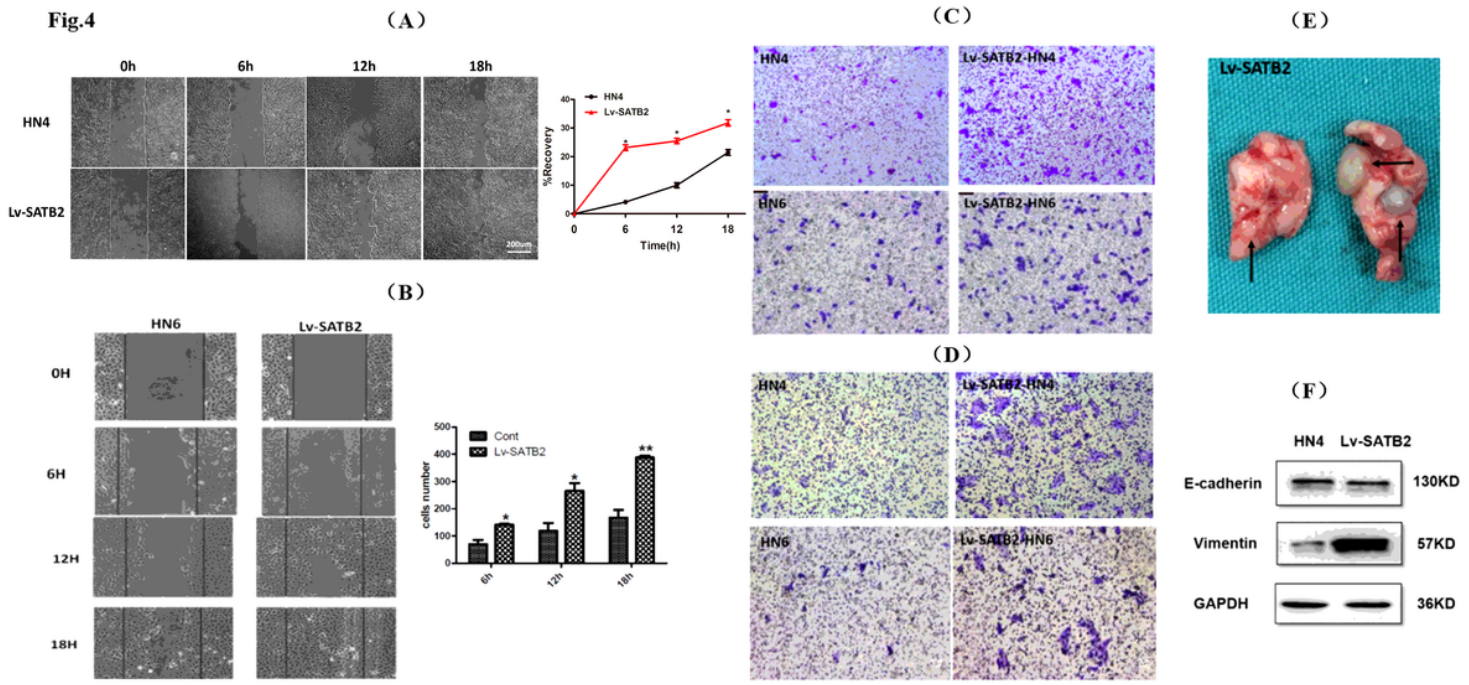

Figure 4

SATB2 promotes migration and invasion in HNSCC and initiates the EMT process. Fig4A,B,C. SATB2 overexpression promotes HNSCC migration as measured by the wound healing test and transwell assay; Fig4D. SATB2 overexpression promotes HNSCC invasion as measured by Matrigel transwell assays Fig4E. Images of mouse lung metastasis from the Lv-SATB2 group 8 weeks after orthotopic injection Fig4F. SATB2 overexpression in HN4 cells initiates EMT process. * $p < 0.05$, ** $p < 0.01$

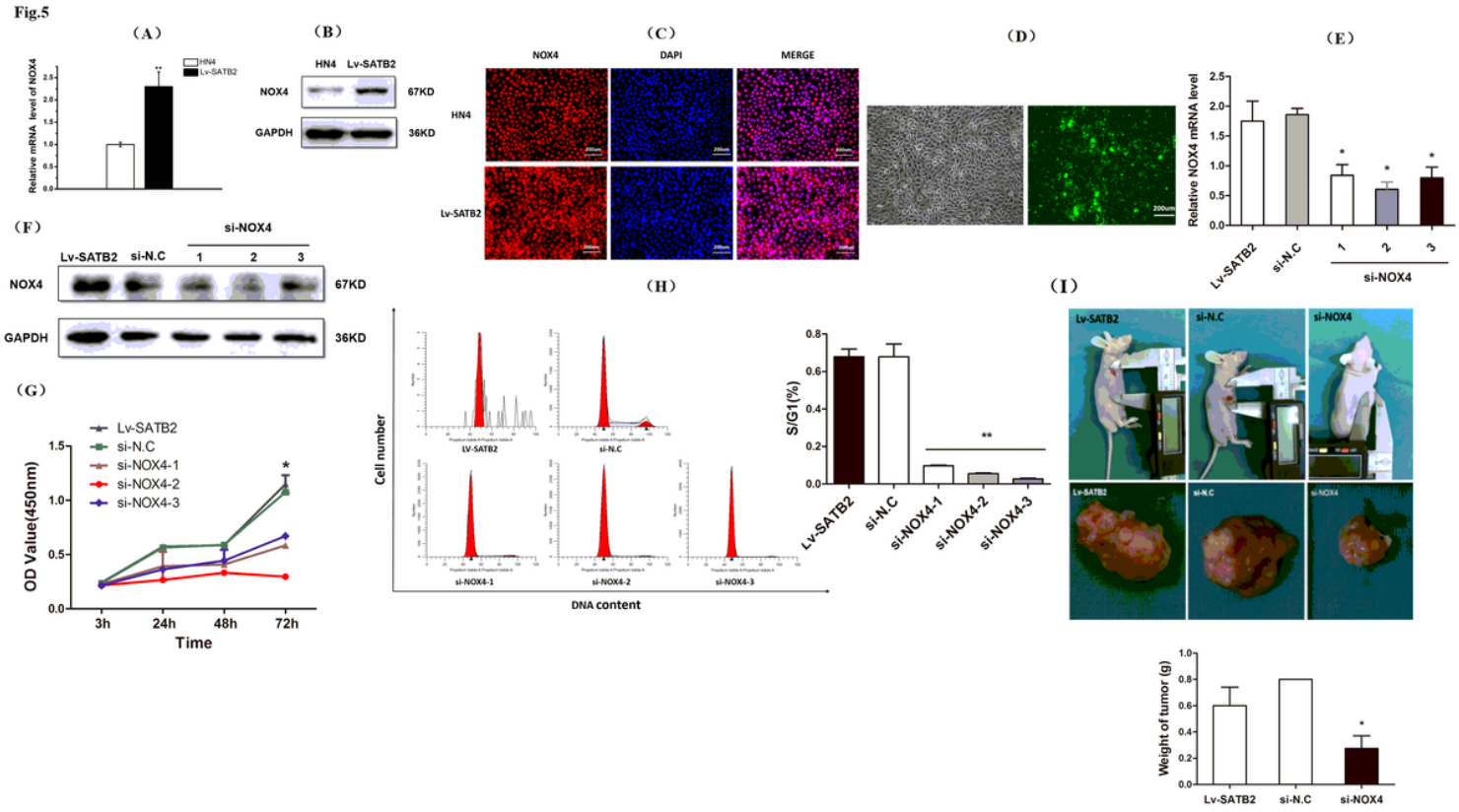

Figure 5

Downregulation of NOX4 suppresses tumor growth caused by SATB2 overexpression. Fig5A-B. Relative NOX4 mRNA and protein levels in HN4 and Lv-SATB2 cells Fig5C. NOX4 enhancement identified by immunofluorescence staining in HN4 and Lv-SATB2 cells * $p < 0.05$ Fig5D. Fluorescence image of Lv-SATB2-HN4 cells transfected with siRNA against NOX4. Fig5E-F.NOX4 mRNA and protein expression levels in HN4 after siRNA transfection. Fig5G. CCK-8 assay shows NOX4 knockdown in Lv-SATB2 cells significantly inhibits proliferation. Fig5H. Cell cycle detection showing that NOX4 down-regulation induces cell cycle arrest at the G1/S checkpoint Fig5I. Tumors measured after 8 weeks' growth in samples harvested from mice injected with NOX4 knockdown and Lv-SATB2 cells.